

# THE INFLUENCE OF A VIAL STOPPER ON FLOW AND MASS TRANSFER CONDITIONS INSIDE A VIAL

MATJAZH HRIBERŠEK, MATEJ ZADRAVEC, ŽIGA ČASAR & JURE RAVNIK

Faculty of Mechanical Engineering, University of Maribor, Slovenia

## ABSTRACT

In the process industry, vacuum-type dryers are becoming increasingly important. A special case of vacuum drying is lyophilization, where a solution, containing up to 90% of solvent (typically water), is dried under the conditions of very low temperatures and extremely low system pressures. As a container type, in which the solution is dried, a vial is frequently used. The intensity of drying is to a large extent controlled by the pressure conditions above the drying surface. The vial and the rubber stopper geometry present a significant pressure drop in the flow of sublimated solvent, but are experimentally difficult to determine. In order to produce realistic pressure conditions for the mass transfer computation, a CFD analysis of flow inside the vial-stopper channel is performed. The influence of imposing the no-slip and slip conditions on the solid surfaces on the pressure drop in the system is studied under the typical sublimation conditions. The effect of the increased partial pressure of the solvent on the sublimation rate is calculated by implementing the Maxwell–Stefan diffusion model.

*Keywords:* computational fluid dynamics, heat and mass transfer, lyophilization.

## 1 INTRODUCTION

Lyophilization as a process of solvent removal takes place under distinct thermodynamic conditions that enable a direct solid–gas phase change – sublimation of the solvent. This means that extremely low system pressure and system temperature are needed in order to avoid the transition of frozen solvent into the liquid state. It is necessary to sustain these conditions during the first or the primary phase of the drying process. As the pressure conditions are mainly the result of the loading of the lyophilizer and capacity and working conditions in the condenser chamber, the temperature in the material in the vial is directly influenced by the balance between the heat, supplied to the vial from the surroundings (trays), and the heat, consumed by the sublimation process at the interface between the frozen material and the already de-iced porous part of the material (Fig. 1).

In recent years, lyophilization modeling was established as a valuable means of improving and optimizing this pharmaceutical production process [1]–[3]. This paper covers the modeling of the first part of the primary drying stage, with the aim to determine the influence of the flow of evaporated solvent from the top of the vial filling to the exit from the vial, which is either open or partially stoppered, on the conditions of mass transfer inside the vial.

## 2 MODELING THE LYOPHILIZATION PROCESS

The freeze-drying process is usually divided into two parts, the primary and secondary drying stage [4]–[6]. The process starts when the frozen substance is subjected to a sudden decrease in system pressure, setting the thermodynamic conditions below the triple point of the solvent (predominantly water) for sublimation to occur. The pressure difference between the sublimation surface and the vacuum induces sublimation, which, due to the sublimation enthalpy, acts as a strong energy sink. Heating of the shelves solves the problem of energy supply and enables taking control of the process. Because of the opened top of the vial, the drying starts at the top and proceeds toward the bottom of the vial. The first stage is therefore represented mainly by the sublimation process of the frozen liquid and it ends when all the frozen water is removed. After the first stage, the second stage begins, where the desorption



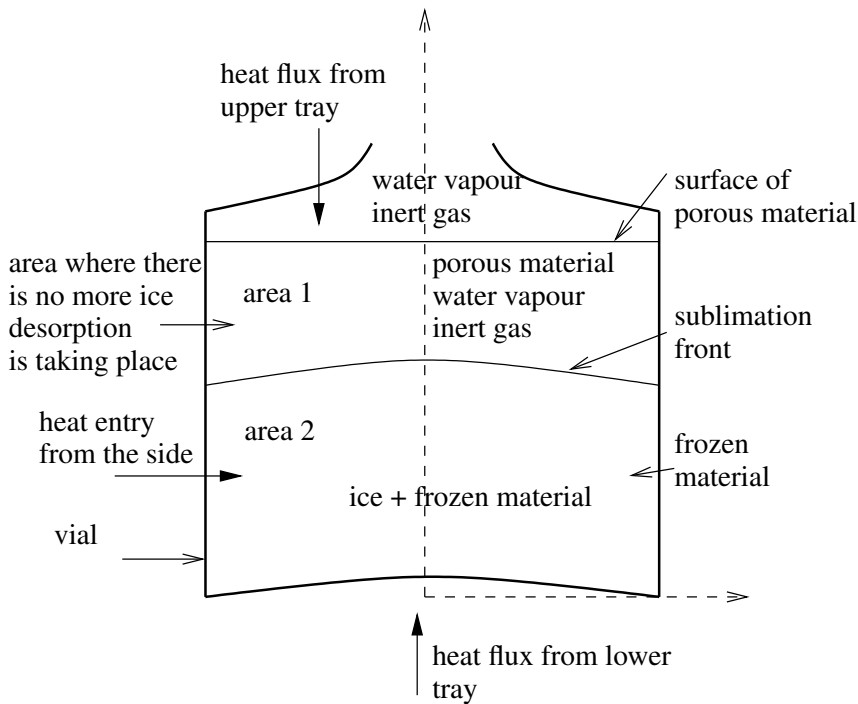


Figure 1: Basic configuration of freeze-drying in a vial [7].

dictates the drying process. The desorption process is also present in the primary drying stage in the dried region, but it is not a dominant process.

This paper covers the modeling of the primary drying stage, with the aim to determine the influence of the stopper on the drying conditions at the surface of the filling at the beginning of the primary drying phase, when the frozen water is directly exposed to the interior of the vial.

## 2.1 Computational model

The freeze-drying process is governed by the mass and energy conservation equations, including the moving interface conditions. In order to obtain the governing set of equations, the energy conservation equation is written for the temperature field in the dried and frozen region, while the mass conservation is usually written for the sublimating water in the form of bounded concentration and partial pressure of liquid vapor, and for the inert gas in the form of partial pressure inside the dried region. The computational algorithm, described in Ravník et al. [6], is an example of an effective model for the solution of the temperature and concentration fields of bounded water inside the substance in the vial, together with the solution of the partial pressure distribution of inert gas and moisture vapor inside the porous layer of the filling.

The boundary conditions for all three variables, temperature, partial pressure of inert gas and of water vapor, depicted in Fig. 2, are set separately for the primary and the secondary

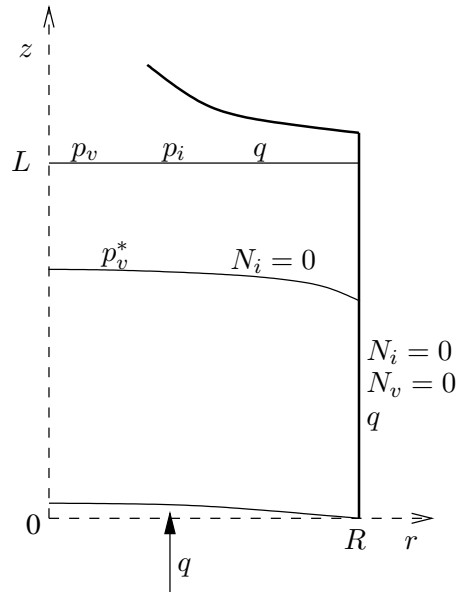


Figure 2: Axisymmetric representation of the vial with boundary conditions.

drying stage. As the focus of this work is on the determination of the correct boundary conditions at the top of the filling, the conditions at the top of  $p_v = 8$  Pa and  $p_i = 4$  Pa are valid for the open vial, without the presence of the stopper, as is usually the case in computer simulations of lyophilization in a vial [5]–[7]. As the stopper is seldom removed from the vial, its presence acts as an additional hydraulic resistance to the flow of the sublimated vapor, leading to increased pressure values for the evaporated solvent at the exit from the vial. As the stopper has a partial opening for the vapor flow when inserted in the vial, the best way to determine the additional flow resistance is by performing a dedicated computational fluid dynamic (CFD) analysis of the vapor flow in the duct, formed by the interior of the vial together with the half-inserted stopper as a typical stopper situation.

## 2.2 Model of surface sublimation

The lyophilization model starts the computation of the conjugate heat and mass transfer in the porous-frozen layer system by setting the initial thickness of the dried region at 2% of the total cake height [5], [7]. A dedicated model for the sublimation of the surface crystals is therefore needed in order to account for the consumed drying time for the initial 2% of the frozen water. Under the assumption that the top layer of ice has approximately the height of 2% of the height of the cake [6], the conditions at the free surface can be approximated as a single layer of ice crystals, and the sublimation model of ice crystals can be designed by considering a direct contact with the gas space of the vial.

The case of sublimating ice crystals can be thus modelled as one-sided diffusion of water vapour from the layer of ice crystals in the direction of the vial opening, in the form of [8]:

$$\vec{J}_v = \frac{C_v}{C_v + C_i} \vec{J}_v - \mathcal{D}_{v,i} \vec{\nabla} C_v.$$

In the direction  $z$ , perpendicular to the ice surface layer the molar flux of vapour is

$$J'_v = \frac{C_v}{C_v + C_i} J'_v - \mathcal{D}_{v,i} \frac{dC_v}{dz}.$$

By considering that the temperature in the interior of the vial fluid volume is not varying significantly, and by using the ideal gas law

$$p_v = C_v RT, \quad (1)$$

the molar flux eqn (1) reads as

$$J'_v = \frac{p_v}{p_v + p_i} J'_v - \frac{\mathcal{D}_{v,i}}{RT} \frac{dp_v}{dz}. \quad (2)$$

The vapour diffusivity in the binary mixture is taken according to Welty et al. [9] as:

$$\mathcal{D}_{v,i} = 0.01883 \frac{\sqrt{T^3 \left( \frac{1}{M_v} + \frac{1}{M_i} \right)}}{(p_i + p_v) \sigma_{vi}^2 \Omega_D}. \quad (3)$$

The Lennard–Jones parameters for the binary mixture are

$$\sigma_{vi} = \frac{\sigma_v + \sigma_i}{2}, \quad \epsilon_{vi} = \sqrt{\epsilon_v \epsilon_i}, \quad (4)$$

with parameter  $\Omega_D$  the collision integral. By inserting eqn (3) into eqn (2), it follows

$$p_i J'_v = -0.01883 \frac{\sqrt{T \left( \frac{1}{M_v} + \frac{1}{M_i} \right)}}{R \sigma_{vi}^2 \Omega_D} \frac{dp_v}{dz}. \quad (5)$$

To get the molar flux, integration is needed from the sublimation surface ( $p_{v,0} = p_v^*$ ) to the top of the vial with conditions of the free space of the lyophilizer drying chamber ( $p_{v,h}$ ),

$$J'_v \int_0^h dz = -0.01883 \frac{\sqrt{T \left( \frac{1}{M_v} + \frac{1}{M_i} \right)}}{p_i R \sigma_{vi}^2 \Omega_D} \int_{p_{v,0}}^{p_{v,h}} dp_v,$$

resulting in the final expression for the molar flux

$$J'_v = -0.01883 \frac{\sqrt{T \left( \frac{1}{M_v} + \frac{1}{M_i} \right)}}{p_i R \sigma_{vi}^2 \Omega_D} \frac{p_{v,h} - p_{v,0}}{h}. \quad (6)$$

With known  $J'_v$ , the time for drying of the first 2% of the cake height ( $\Delta h$ ) can be computed as:

$$\Delta t = \frac{\rho_1 \Delta h}{M_v J'_v}. \quad (7)$$



### 2.3 Fluid flow model

In order to obtain the pressure drop that occurs within the vial and the stopper geometry, a CFD analysis was performed. The ideal way of performing the CFD analysis would be by a direct coupling of heat and mass transfer computation of the process inside the vial filling, by using a dedicated computational model [6], [7] and a full 3D CFD analysis of vapor flow through the interior vial duct with the stopper. As this would require the derivation of a new computer program, a simplified approach was adopted. The chosen approach is based on a decoupled analysis of both phenomena, whereas the initial mass flow of sublimated vapor, obtained for the sublimation mass flow scenario, that occurs in the pure free-surface sublimation, was used as the boundary condition for the CFD analysis. The governing equations solved by the CFD code (Ansys-CFD code CFX [10]) were:

$$\vec{\nabla} \cdot \vec{u} = 0, \quad (8)$$

$$(\vec{u} \cdot \vec{\nabla})\vec{u} = -\frac{1}{\varrho}\vec{\nabla}p + \nu\Delta\vec{u}, \quad (9)$$

where  $\vec{u}$  is the gas velocity,  $\nu$  kinematic viscosity,  $\varrho$  gas density and  $p$  pressure. However, due to extremely low system pressure in a typical sublimation process, the rarified gas effects can play an important role. Therefore, as the system pressure is extremely low, the effect of velocity slip at the solid walls was additionally evaluated within the CFD computations.

The boundary conditions for the sublimation surface were as follows: the maximum mass flow rate, obtained from experimental data in [7], was set at the sublimation surface. The outlet from the domain was set at one vial diameter distance from the centerline of the vial, in order to allow exiting of the vapor from the interior of the vial. The reference system pressure was set at 4 Pa, hence the difference between the computed pressure level at the sublimation surface, and the exit of the vial can be taken as the valid pressure drop inside the vial-stopper system. As in the case of rarified gas flow, where the velocity slip occurs at the solid walls, two test cases were considered: the *no-slip* case with prescribed zero velocity at the solid walls, and the *free-slip* case with a zero shear stress condition at the solid wall. The latter conditions can be viewed as an extreme case of the rarified gas flow, where the solid wall in the tangential direction does not influence the flow of fluid. The vial under consideration, denoted by A20-C13, had an inner diameter of 20 mm, a height of 45 mm and an opening diameter of 12.6 mm.

## 3 RESULTS AND DISCUSSION

The computed pressure field inside the vial and its development through the stopper opening is shown in Fig. 3. The influence of the stopper is clearly visible, as the local velocity at the exit from the stopper increases significantly with regard to the condition in the vial throat. For the case of the free-slip conditions, this effect is still evident, although the peak velocities are approximately 10% lower. In order to evaluate the effect of the stopper, the case of the A20-C13 vial without inserted stopper was also computed. From the comparison of pressure distribution along the centreline of the vial (Fig. 4), one can conclude that the presence of the stopper increases the pressure inside the vial significantly.

From the pressure distribution along the centreline of the vial, one can now determine the pressure level at the exit from the vial (at  $y = 0.042$  m for A20-C13) and consequently the pressure difference between the sublimation surface and the exit from the vial. The value of the pressure at the vial outlet and consequently the new outlet boundary condition for computation of the drying time, eqn (7), is therefore:



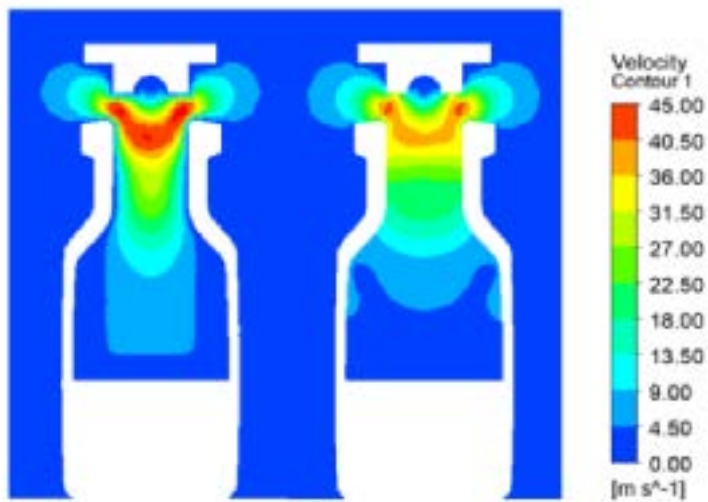


Figure 3: Pressure distribution inside the vial with inner diameter of 20 mm: no-slip boundary condition (left), slip boundary condition (right).

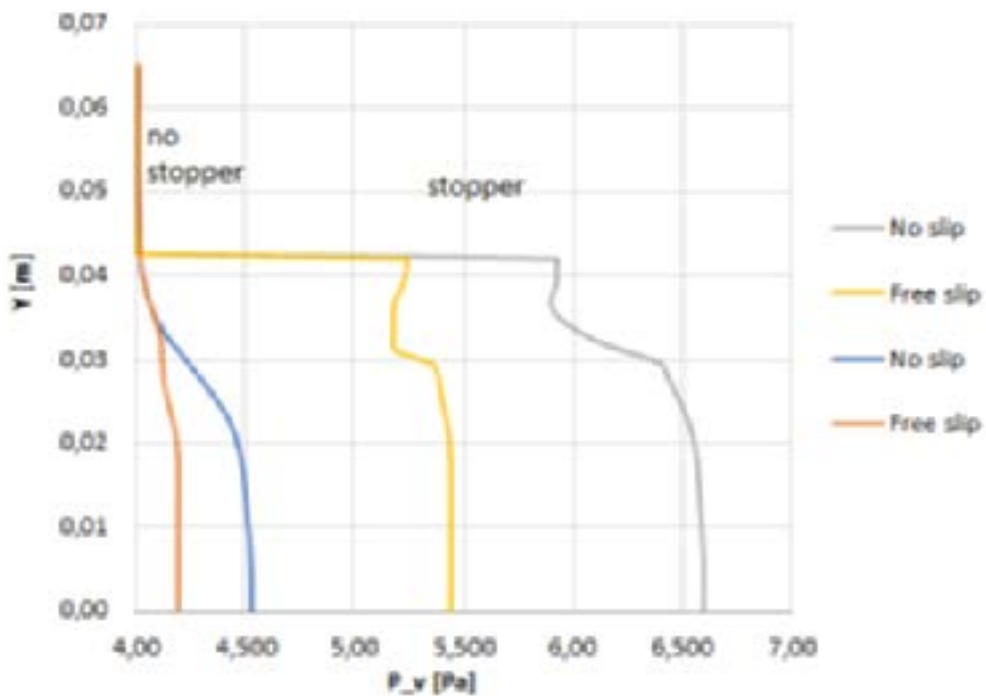


Figure 4: Pressure distribution inside the vial with inner diameter of 20 mm: no-slip boundary condition (left), slip boundary condition (right).

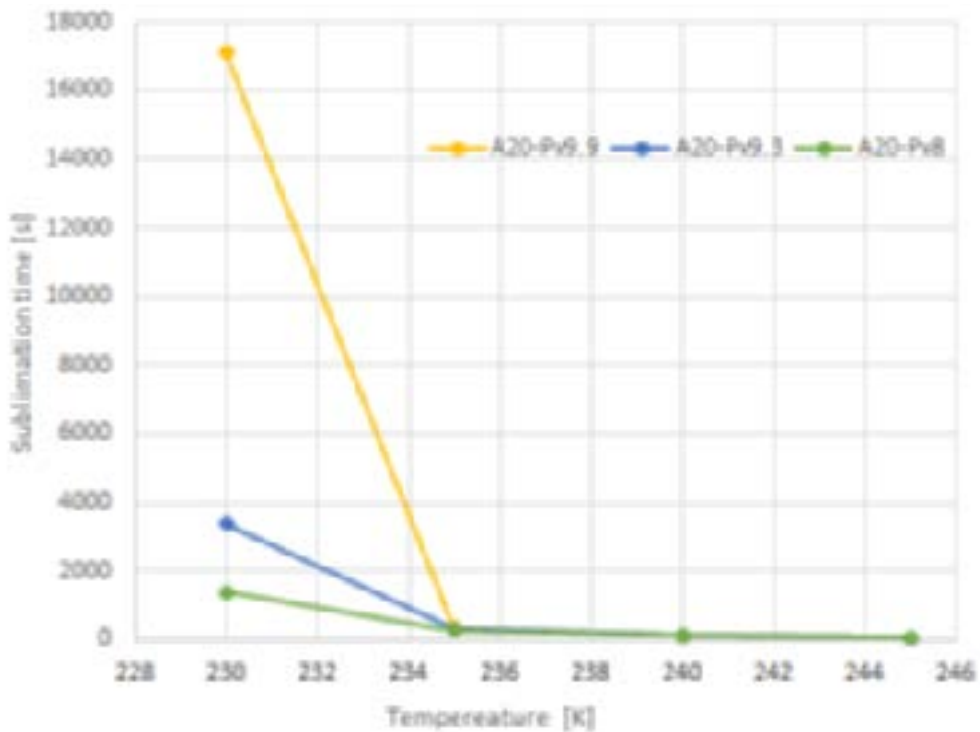


Figure 5: Drying time for sublimation of the upper ice layer for different system conditions.

- for the case of the vial with inner diameter of 20 mm without considering the pressure increase inside the vial:  $p_{v,h} = 8.0$  Pa;
- for the case of the no-slip boundary condition:  $\Delta p_v = 1.9$  Pa; resulting in the  $p_{v,h} = 9.9$  Pa;
- for the case of the free-slip boundary condition:  $\Delta p_v = 1.3$  Pa, resulting in the  $p_{v,h} = 9.3$  Pa.

The increase in outlet pressure results in the significant increase of drying time, computed by using eqn (7), needed for the sublimation of the upper 2% of the filling (see Fig. 5). The additional data for computation were:  $M_i = 29$  kmol/kg,  $M_v = 18$  kmol/kg,  $T = 230$  K,  $p_i = 4$  Pa,  $R = 8314$  J/kmol K,  $\sigma_{v,i} = 3.754$  Å,  $\Omega_D = 0.9332$ .

In the case of the highest outlet pressure, the drying time increases by a factor of more than 10. This is not a surprise, as the sublimation vapor pressure at the surface of the ice at 230 K is 10.1 Pa; therefore, the pressure difference, driving the sublimation process, is close to being zero. When increasing the sublimation temperature, the drying accelerates; however, in production, the increase of sublimation temperature is modest and occurs when the sublimation front is already well inside the partially dried cake. In this case the sublimation vapor pressure increase is counterbalanced by the increased solvent vapor pressure in the porous region, which now presents the most important mass transfer resistance in the vial; hence, the fully coupled system of heat and mass transfer governing equation for the moving phase change problem, [7], [6] has to be implemented.

## 4 CONCLUSIONS

It is well known that without the additional heat from the shelf, that compensates for the sublimation enthalpy and then also increases the temperature inside the vial, which in turn increases the pressure level at the sublimation surface, the lyophilization process could not be performed with production-relevant cycle times. However, the pressure increase inside the vial also leads to an increase in drying time, as the pressure difference, which drives the sublimation, decreases, and should not therefore be neglected when setting the correct outlet pressure boundary conditions for computation of the lyophilization process inside the vial.

## REFERENCES

- [1] Brulls, M. & Rasmuson, A., Heat transfer in vial lyophilization. *International Journal of Pharmaceutics*, **246**, pp. 1–16, 2002.
- [2] Gan, K.H., Bruttini, R., Crosser, O.K. & Liapis, A.I., Heating policies during the primary and secondary drying stages of the lyophilization process in vials: Effects of the arrangement of vials in clusters of square and hexagonal arrays on trays. *Drying Technology*, **22**, pp. 1539–1575, 2004.
- [3] Daraoui, N., Dufour, P., Hammouri, H. & Hottot, A., Model predictive control during the primary drying stage of lyophilisation. *Control Engineering Practice*, **18**, pp. 483–494, 2010.
- [4] Pikal, M.J., Roy, M.L. & Shah, S., Mass and heat transfer in vial freeze-drying of pharmaceuticals: Role of the vial. *Journal of Pharmaceutical Sciences*, **73**(9), pp. 1224–1237, 1984.
- [5] Mascarenhas, W.J., Akay, H.U. & Pikal, M.J., A computational model for finite element analysis of the freeze-drying process. *Computer Methods in Applied Mechanics and Engineering*, **148**, pp. 105–124, 1997.
- [6] Ravnik, J., Golobič, I., Sitar, A., Avanzo, M., Irman, Š., Kočevár, K., Cegnar, M., Zadavec, M., Ramšak, M. & Hriberšek, M., Lyophilization model of mannitol water solution in a laboratory scale lyophilizer. *Journal of Drug Delivery Science and Technology*, **45**, pp. 28–38, 2018.
- [7] Ramšak, M., Ravnik, J., Zadavec, M., Hriberšek, M. & Iljaž, J., Freeze-drying modeling of vial using BEM. *Engineering Analysis with Boundary Elements*, **77**, pp. 145–156, 2017.
- [8] Bird, R.B., Stewart, W.E. & Lightfoot, E.N., *Transport Phenomena*, 2007.
- [9] Welty, J., Wicks, C., Wilson, R. & Rorrer, G., *Fundamentals of Momentum, Heat, and Mass Transfer*, John Wiley and Sons, 2008.
- [10] Ansys CFD, *CFX 17.0*, 2016.

